iScience

CellPress

Article

Adaptive Diversification of the Lateral Line System during Cichlid Fish Radiation

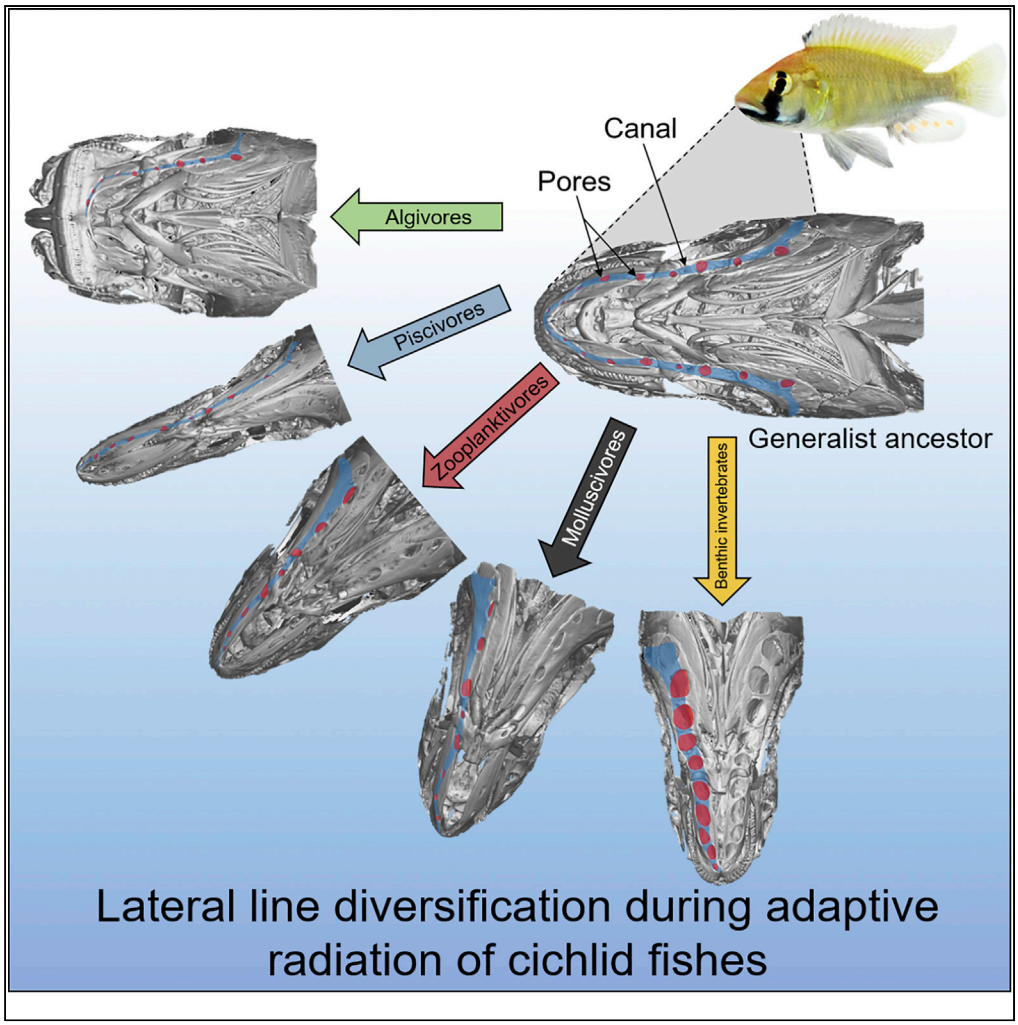

Duncan E. Edgley, Martin J. Genner

duncan.edgley@bristol.ac.uk (D.E.E.)
m.genner@bristol.ac.uk (M.J.G.)

HIGHLIGHTS

Lateral line system shows considerable diversity in Lake Malawi cichlids

Diet is strongly associated with cranial lateral line morphology

Lateral line specialization may promote cichlid fish adaptive radiation

Edgley & Genner, iScience *16*, 1–11
June 28, 2019
https://doi.org/10.1016/j.isci.2019.05.016

iScience

CellPress

Article

Adaptive Diversification of the Lateral Line System during Cichlid Fish Radiation

Duncan E. Edgley[1,2,*] and Martin J. Genner[1,*]

SUMMARY

The mechanosensory lateral line system is used by fishes to sense hydrodynamic stimuli in their environment. It provides information about flow regimes, proximity to substrate, and the presence and identity of prey and predators and represents a means of receiving communication signals from other fish. Thus we may expect lateral line system structures to be under strong divergent selection during adaptive radiation. Here, we used X-ray micro-computed tomography scans to quantify variation in cranial lateral line canal morphology within the adaptive radiation of Lake Malawi cichlids. We report that cranial lateral line canal morphology is strongly correlated with diet and other aspects of craniofacial morphology, including the shape of oral jaws. These results indicate an adaptive role for the lateral line system in prey detection and suggest that diversification of this system has taken an important role in the spectacular evolution of Lake Malawi's cichlid fish diversity.

INTRODUCTION

The lateral line system is an important mechanosensory system used to detect hydrodynamic stimuli in aquatic environments (Webb, 2014; Klein and Bleckmann, 2015). It is found in all fishes, including lampreys, and some amphibians (Gelman et al., 2007; Schlosser, 2012), indicating that it may be a primitive vertebrate character. In teleost fishes, it comprises two key components with separate receptive abilities: the superficial neuromasts and the canal neuromasts (Bleckmann and Zelick, 2009). The superficial neuromasts, present on the surface of the fish, are thought to assess direct current and are used for sensing the direction and speed of water flow (Bleckmann and Zelick, 2009; Wark and Peichel, 2010). Canal neuromasts are situated within fluid-filled canals between skeletal openings (pores) and are thought to be more important for detecting pulses in water movement, such as those associated with the movement of other organisms (Montgomery et al., 1994; Coombs et al., 2001), against background noise (Engelmann et al., 2000) (Figure 1). A widened lateral line canal phenotype, accompanied with increased pore size, is thought to convey increased sensitivity to certain hydrodynamic stimuli (Webb, 2014; Klein and Bleckmann, 2015: Schwalbe and Webb, 2015). Collectively, the transduction of flow stimuli through the superficial and canal neuromasts is thought to inform multiple key behaviors in fishes, including rheotaxis (Montgomery et al., 1997; Kulpa et al., 2015), prey detection (Montgomery and McDonald, 1987; Janssen, 1996; Pohlmann et al., 2004; Schwalbe et al., 2012), predator avoidance (Stewart et al., 2014), shoaling behavior (Faucher et al., 2010), and male-male competition (Butler and Maruska, 2015). Thus we may expect them to have been subject to strong divergent selection during adaptive radiation into multiple ecologically and behaviorally distinct species.

Cichlid fishes are one of the largest and most diverse of all vertebrate families, comprising over 3,000 species (Seehausen, 2006; Salzburger, 2018) and reaching their highest diversity in the Great Rift Valley lakes of East Africa (Seehausen 2006, 2015). The Lake Malawi haplochromine radiation alone comprises over 500 species that have evolved from common ancestry within the last 1.1 Ma (Malinsky and Salzburger, 2016; Malinsky et al., 2018). These cichlids have diversified extensively in habitat preferences, diet, body shape, craniofacial morphology related to prey capture and processing (Turner, 1996; Albertson et al., 2003; Konings, 2016), breeding behaviors (Konings, 2016; York et al., 2018), and sensory abilities, notably vision (Parry et al., 2005). However, knowledge of their lateral line system diversification is limited to (1) anatomical work that has shown variation among genera in the size and development of cranial canal morphology (Eccles and Trewavas, 1989; Schwalbe et al., 2012; Bird and Webb, 2014; Becker et al., 2016) and (2) behavioral work showing that two Lake Malawi species with differences in cranial canal morphology differ in their ability to locate live prey in dark environments (Schwalbe et al., 2012; Schwalbe and Webb, 2015). Thus we

[1]School of Biological Sciences, University of Bristol, Life Sciences Building, 24 Tyndall Avenue, Bristol BS8 1TQ, UK

[2]Lead Contact

*Correspondence: duncan.edgley@bristol.ac.uk (D.E.E.), m.genner@bristol.ac.uk (M.J.G.)

https://doi.org/10.1016/j.isci.2019.05.016

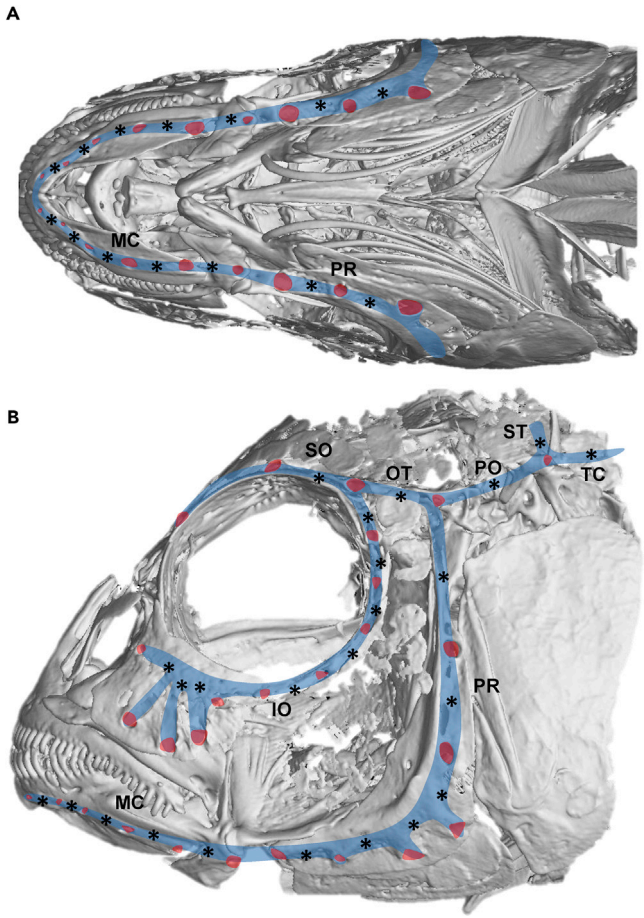

Figure 1. Overview of the Cranial Canal Lateral Line System of the Lake Malawi Cichlid *Astatotilapia calliptera*

(A and B) (A) Ventral view and (B) lateral view. The positions of canals (blue) and pores (red) are shown. Approximate position of canal neuromasts are shown as asterisks. MC, mandibular canal; PR, preopercular canal; SO, supraorbital canal; IO, infraorbital canal; OT, otic canal; PO, post-otic canal; ST, supratemporal canal; TC, trunk canal. Positioning of canal neuromasts is from staining of *A. calliptera* with DASPEI, corroborated with evidence from Butler and Maruska (2015) who studied the congeneric *Astatotilapia burtoni*.

conducted the first large-scale comparative study of lateral line system morphology across the phylogenetic and ecomorphological diversity of an African cichlid radiation and tested for interspecific associations between morphology and ecological variables.

RESULTS AND DISCUSSION

Lateral Line Morphology and Head Shape Covary

We focused our analysis on the lateral line canal components of the head and used X-ray micro-computed tomography scans to study lateral and ventral views of cranial morphology, including the size and position of cranial canal pores (Figure S2; Table S2). We quantified cranial lateral line system variation among 52 species of Lake Malawi cichlids using landmark-based geometric morphometrics (Figures 2, S2, and S3; Table S1) and tested for associations with gross morphology and ecology using distance-based redundancy analysis (Legendre and Anderson, 1999). We initially found that variation in cranial lateral line pore morphology was strongly coupled with variation in gross cranial morphology (Figures 3A–3C). For example, larger pores were associated with longer and broader jaw bones (Figures 4A–4C, 5A, and 5B). Previous work has demonstrated considerable modularity of the cichlid skull, including a major preorbital module that encompasses both the upper and lower oral jaws (Parsons et al., 2011). Our findings suggest that the cranial lateral line canal system is an intrinsic part of this more complex preorbital module. Although oral jaws have typically been considered to have a primary role in the handling and processing of prey in cichlid fishes (Turner, 1996; Albertson et al., 2003; Hulsey and García de

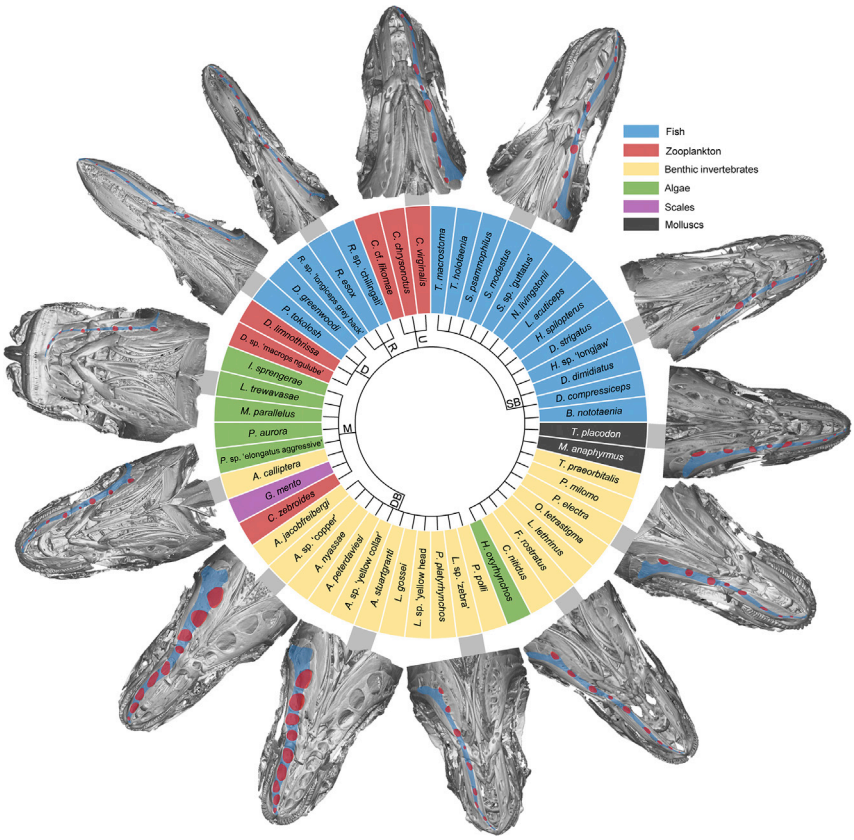

Figure 2. The Diversity of Cranial Lateral Line Canal Morphology Among the Lake Malawi Cichlid Species Included in Our Study

Individuals are grouped into the six major evolutionary lineages (Malinsky et al., 2018) and color coded by dietary preference. Micro-computed tomographic images are not to scale. The positions of pores (red) and approximate position of canals (blue) are shown on the left side of each fish. R, *Rhamphochromis*; D, *Diplotaxodon*; U, utaka; SB, shallow benthic; DB, deep benthic; M, mbuna. A full list of species is provided in Table S1 and Figure S1.

León, 2005; Muschick et al., 2011; Parsons et al., 2012; Konings, 2016), these results additionally highlight a role for the lateral line canals of the lower jaw in hydrodynamic sensing of prey.

Diet Predicts Cranial Lateral Line Morphology

Our results demonstrated dietary grouping to be a significant predictor of both ventral and orbital canal morphologies (Figures 3B and 3C), but not preopercular canal morphology (Figure 3A). This is notable as canals in the ventral and orbital regions can be considered to have ventral- (or anterior-) facing pores (Figures S2A and S2C). Specifically, the ventral view of the head encompassed the ventral-facing mandibular canal and ventral arm of the preopercular canal (Figures 1A and S2A), whereas the orbital lateral line pore morphology we measured encompassed primarily anterior-/ventral-facing pores, including the infraorbital canal within the lacrimal bone (Figures 1B and S2C). In contrast, the pores of the preopercular canal can be considered to be more lateral facing (Figures 1B and S2B). Anterior- or ventral-facing pores have been proposed to be functional during feeding behavior, specifically in relation to the observed "sonar" feeding by wild *Aulonocara* and other benthic genera, where foraging fish angle their body and probe for cryptic buried prey (Turner, 1996; Schwalbe et al., 2012; Konings, 2016). Our results are therefore supportive of this proposed role for the cranial lateral line in prey detection.

Benthic invertebrate feeders and molluscivores appear to have the largest cranial canal pores (Figures 4A–4C), consistent with widened canals and enlarged pores associating with detection of cryptic prey within the substrate (Turner, 1996; Schwalbe et al., 2012; Konings, 2016). Behavioral trials in light-limited

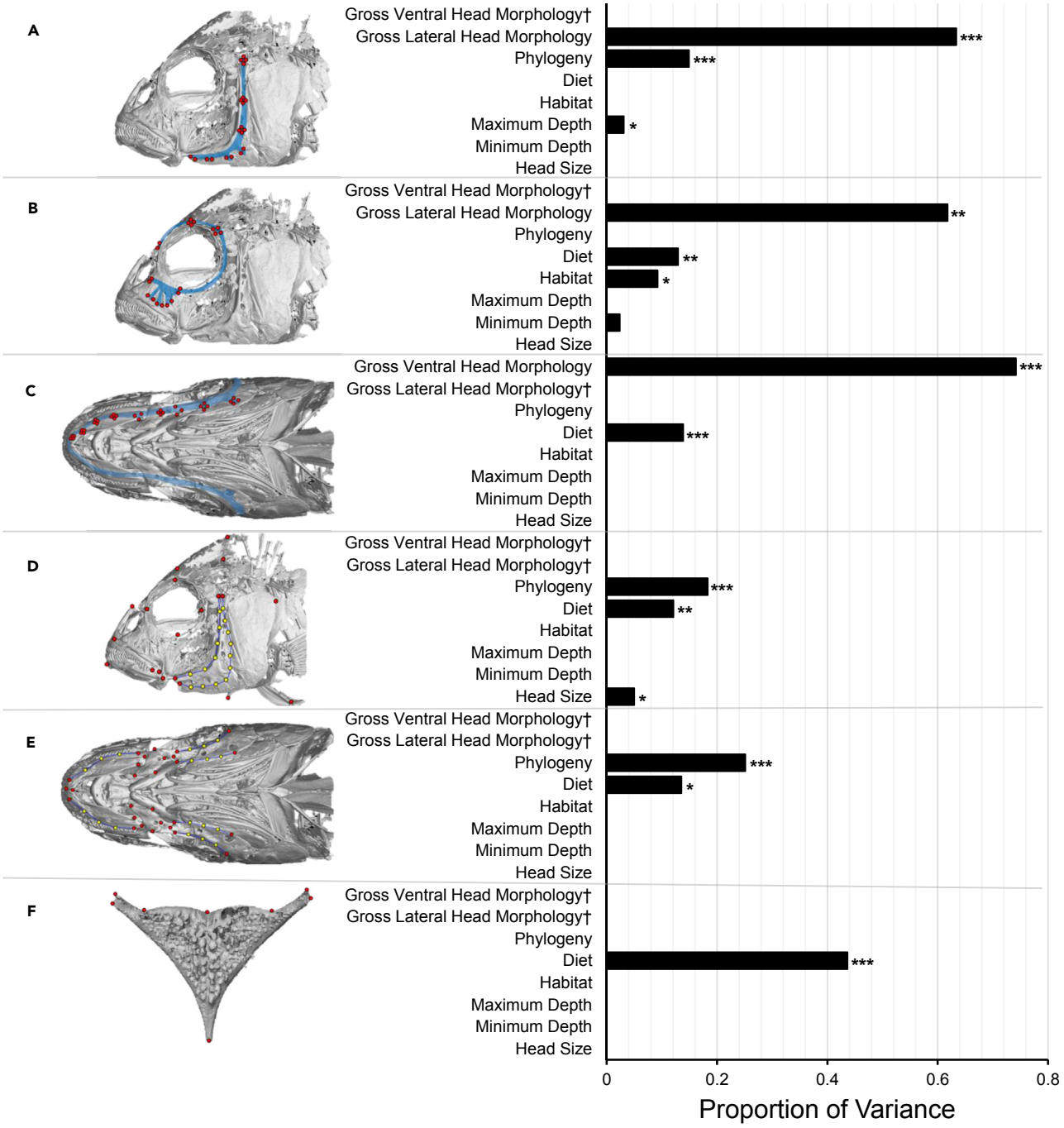

Figure 3. The Proportion of Variance in Morphology Explained by Each Morphological or Ecological Explanatory Variable, Calculated through Distance-Based Redundancy Analysis and Analysis of Variance

(A–F, left) Sets of landmarks used as independent variables for our analysis, illustrated on micro-computed tomographic images of *Astatotilapia calliptera*. Red dots are landmarks, and yellow dots are semi-landmarks. Semi-landmarks slide along blue lines between landmarks. Approximate canal positioning is illustrated in blue. Full explanation of landmarks is provided in Figure S2.

(A–F, right) Proportion of variance in morphology explained by each explanatory variable as calculated through distance-based redundancy analysis. †Variable omitted from model; *$p < 0.05$; **$p < 0.01$; ***$p < 0.001$.

(A) Preopercular lateral line pore morphology.

(B) Orbital (infra- and supraorbital) lateral line pore morphology.

(C) Ventral head lateral line pore morphology.

Figure 3. *Continued*
(D) Gross lateral head cranial morphology.
(E) Gross ventral head cranial morphology.
(F) Lower pharyngeal jaw morphology.

environments have shown that *Aulonocara stuartgranti*, a species with large pores, is able to forage more effectively on live arthropod prey than *Tramitichromis* sp., which possesses comparatively smaller pores and narrower canals (Schwalbe and Webb, 2015). Our results emphasize the need to further explore the limits of benthic prey detection associated with the range of lateral line morphologies of these cichlids, ideally focusing on natural prey items and substrates mirroring those present in Lake Malawi. Our results also reveal variation among other trophic groups, with variation in pore size and positioning present in piscivores, zooplanktivores, and herbivores (Figures 4A–4C).

Diet was also a significant predictor of the variation in gross cranial morphology, which covaried extensively with the cranial lateral line canal morphology (Figures 3D–3F). Species in each dietary grouping had a combination of traits specific to those diets. For example, molluscivores tended to have shorter downward-facing oral jaws and more robust pharyngeal jaws, piscivores had more elongated forward-facing oral jaws and narrower pharyngeal jaws, and benthic algivores had short downward-facing oral jaws coupled with relatively robust pharyngeal jaws (Figures 5A–5C). The fin biter and scale eater *Genyochromis mento* was unique in possessing wide, but short oral jaws (Figures 5A–5C). We note that the elongated jaw phenotype of piscivores and the broad jaw phenotype of algivores (Figures 5A and 5B) were both paired with a relatively small pore size (Figures 4A–4C), whereas the relatively large pores of benthic invertebrate feeders tended to be coupled with widened preopercular bones in particular (Figures 5A and 5B). Our results confirmed our expectations of an association between lower pharyngeal jaw morphology and diet in Malawi cichlids (Figures 5C and 3F), as has been shown in Tanganyika cichlid fishes (Muschick et al., 2011). This is important in the context of this study as it demonstrates that our methods are reliably able to recover functional associations between diet and morphology. Taken together, our results are supportive of natural selection being a major driver of cranial ecomorphological diversification in cichlids, with selection on traits related to the detection of hydrodynamic stimuli produced by prey being an important yet largely overlooked component of this diversification process.

Lateral Line Diversification Is Partially Independent of Phylogenetic Constraint

Recent work has confirmed that phylogeny corresponds closely with previously defined ecomorphological groupings (Genner and Turner, 2012) across the endemic Lake Malawi haplochromines (Malinsky et al., 2018) (Figure S1). We included representatives of all the major lineages known to comprise the radiation, including open water piscivores (*Rhamphochromis*), deep water predators (*Diplotaxodon-Pallidochromis*), open water zooplanktivores (utaka), shallow water rock cichlids (mbuna), the typically shallow water sediment-associated cichlids (shallow benthic), and the typically deep water sediment-associated cichlids (deep benthic). For our analyses we placed the shallow water generalist *Astatotilapia calliptera* within the mbuna grouping, given their recent shared evolutionary history (Malinsky et al., 2018) (Figure S1).

When previous adaptation limits future evolutionary pathways despite the presence of strong selection pressures we may consider an evolutionary lineage to be phylogenetically constrained (McKitrick, 1993). For example, in the context of cichlid fishes, it may be possible for some taxa possessing broad oral jaw bones to develop larger pores as a sensory specialization for feeding on motile benthic prey. Other taxa with narrow oral jaw bones may be unable to follow this evolutionary trajectory. It is notable that no species within the mbuna, *Rhamphochromis*, or *Diplotaxodon* lineages have widened lateral line canal phenotypes (Figures 2 and 4). We suggest that constraints conferred by head shape including the thin, laterally compressed piscivore phenotype, and the flat, anteroposteriorly compressed algivore phenotype (Figures 5A and 5B), may both prevent the evolution of broad preopercular and mandibular bones and hence also prevent the evolution of widened canals and pores. Such phylogenetic constraints would manifest in traits associating more strongly with phylogenetic grouping than with ecology. Our results showed that both gross cranial morphology (Figures 3D and 3E and S2D) and preopercular lateral line pore morphology (Figures 3A and S2B) were significantly associated with phylogenetic grouping. However, this was not the case for both the diet-associated ventral and infraorbital cranial canal pore morphologies (Figures 3A, 3B, S2A, and S2C). These results indicate that diet-associated traits are able to diversify somewhat independent of phylogenetic constraint and is further suggestive of the lateral line system being under selection during rapid adaptive radiation.

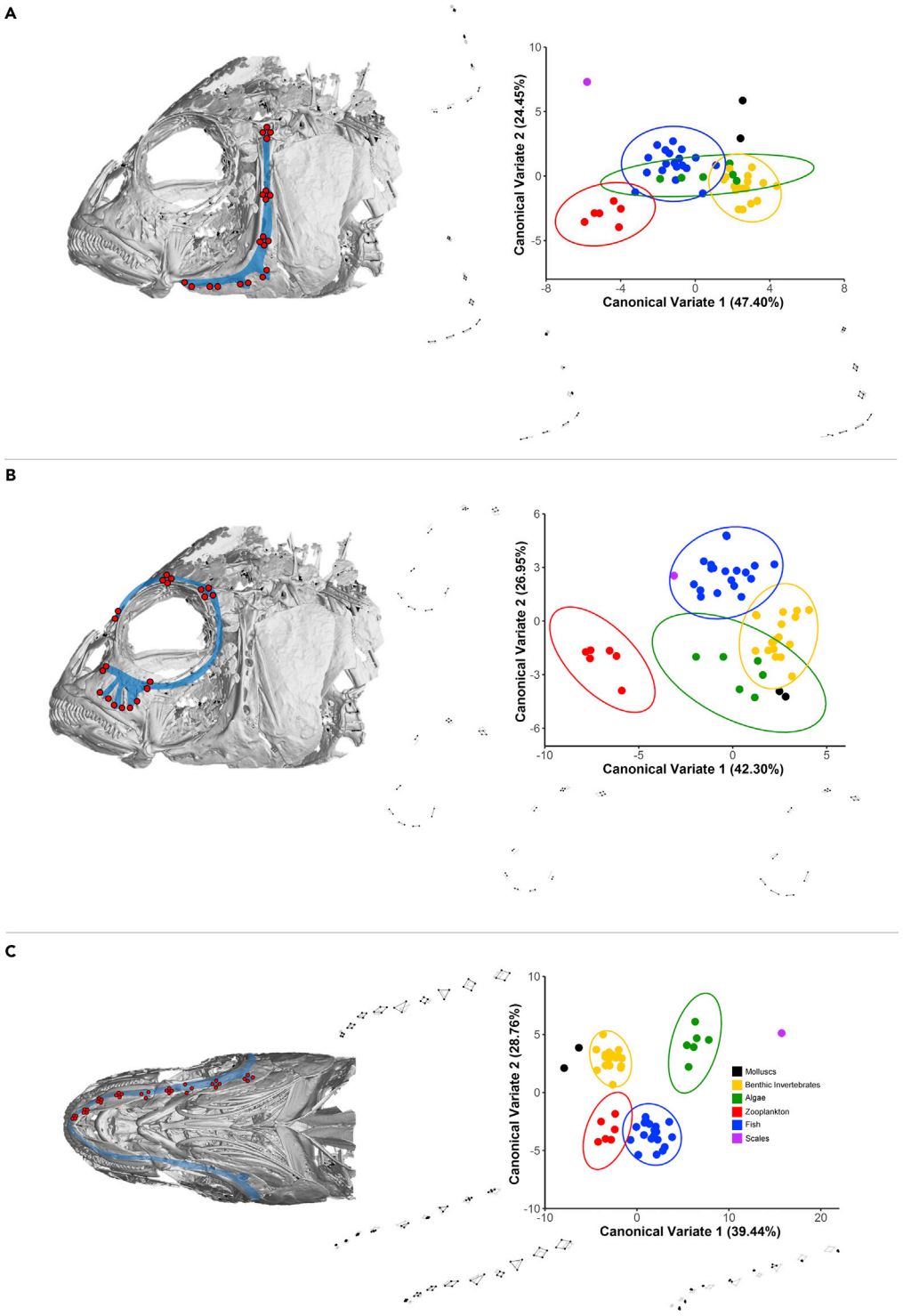

Figure 4. Variation in Cranial Lateral Line Pore Morphology Observed Among Dietary Groupings within the Lake Malawi Haplochromine Radiation

(A–C, left) Arrangements of landmarks used in our analysis illustrated on micro-computed tomographic images of *Astatotilapia calliptera*. Red dots represent landmarks, and the approximate positioning of the relevant lateral line canals are shown in blue. Full explanation of landmark positioning is provided in Figure S2.

(A–C, right) Variation in morphology of cranial lateral line pores among our 52 study specimens. Variation is shown for each landmark set, calculated using canonical variates analysis, displaying canonical variate (CV) scores on the first two

Figure 4. *Continued*

axes. Individuals are grouped by diet, and for CV scores, 95% confidence ellipses are shown for all dietary groupings with n > 2. Changes in landmark arrangement associated with each axis are illustrated on wireframe graphs (Klingenberg, 2013). Wireframe graphs along each axis show consensus landmark arrangement for the 52 species (gray dots and lines) and landmark position shifts associated with each CV axis (black dots and lines). The two wireframe graphs on each axis illustrate changes in landmark positioning associated with the highest and lowest values for each CV on that axis (black dots and lines).

(A) Preopercular lateral line pore morphology.

(B) Orbital (infraorbital and supraorbital) lateral line pore morphology.

(C) Ventral head lateral line pore morphology.

Associations with Depth and Habitat

Research on the lateral line systems within the Lake Malawi radiation has highlighted a contrast between the "widened" canals or pores of a dark-adapted benthic genus (*Aulonocara*) and the relatively "narrow" canals and pores of a shallow water genus (*Tramitochromis*) (Schwalbe et al., 2012). Our analyses show for the first time that depth (and hence light level) does not consistently predict this morphology (Figures 4B and 4C). For example, shallow-living species such as the benthic arthropod feeding *Fossorochromis rostratus* and the mollusc-specialist *Trematocranus placodon* also have relatively large mandibular and preopercular canal pores (Figures 2 and 4A–4C). Given that these species are commonplace in clear water soft-sediment littoral habitats, we suggest that a range of benthic invertebrate feeders may use motion cues for location of prey within the sediment, independent of depth and light levels.

Habitat was not a consistent predictor of either gross craniofacial morphology or cranial lateral line canal morphology in our analyses. This may in part be related to the cranial lateral line system being useful for sensing benthic prey multiple habitat types, as indicated by cichlid genera with enlarged cranial lateral line canal pores occupying a range of habitats. For example, *Aulonocara* are found in both deep water soft-sediment habitats (e.g., *Aulonocara* sp. "copper") (Turner, 1996) and in shallow water cave-like habitats (e.g., *Aulonocara jacobfreibergi*) (Konings, 2016). The decoupling of lateral line morphology and habitat may also reflect the diversity of trophic-specialist taxa present within each of the habitats. For example, a rich diversity of piscivores and zooplanktivores are found in soft-sediment habitats along with benthic invertebrate feeding species (Turner, 1996; Konings, 2016). Given the range of potential diets within each habitat type, an equivalent diversity of corresponding craniofacial morphologies would be predicted to be present within each to enable the detection, capture, and processing of available prey items.

Modularity and the Cranial Lateral Line System

The degree of modularity within a skeletal system is thought to either constrain or facilitate rapid evolutionary divergence (Pugliucci, 2008; Parsons et al., 2011, 2012; Bird and Webb, 2014). The bones of the preorbital region of the cichlid head, which comprises the oral jaws and supporting structures, form a functional module (Cooper et al., 2010; Parsons et al., 2011). This module has limited axes of variation available during adaptation to specific trophic resources (Parsons et al., 2012), which is perhaps one contributing factor to the striking parallel evolution of craniofacial morphology present among the Lake Malawi, Lake Victoria, and Lake Tanganyika cichlid radiations (Young et al., 2009).

Our study has shown covariance between jaw morphology and aspects of lateral line morphology, such as the positioning of pores, when the Lake Malawi radiation is considered as a whole. However, our study also confirms observations that species with very distinct jaw phenotypes can possess similar narrow canal phenotypes, demonstrating that cranial lateral line morphology can decouple from gross jaw morphology (Bird and Webb, 2014). Detailed comparative analysis of cichlid canal phenotypes has demonstrated that the phenotypic differences observed among large-pored and small-pored species can largely be attributed to rate heterochrony (Bird and Webb, 2014; Webb et al., 2014). Thus future studies concentrating on the evolution of interspecific variation in lateral line morphology should have a strong focus on the relative rate of phenotypic development among taxa.

Concluding Remarks

Our study provides insights into the scale of cranial lateral line system variation across a major vertebrate adaptive radiation. We provide quantitative evidence showing that cranial canal lateral line pore morphology covaries with gross oral jaw morphology, and that additional variation is explained by species

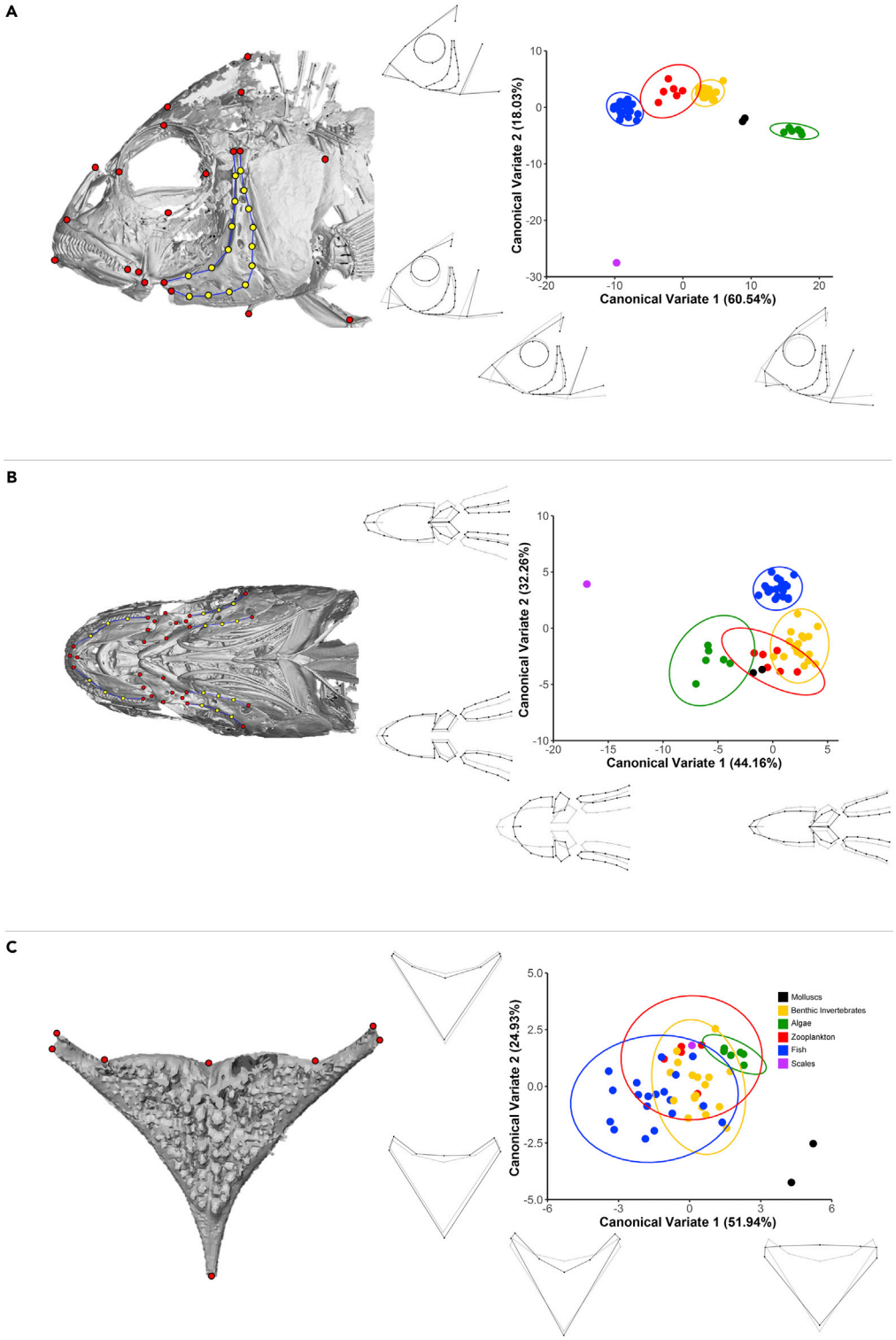

Figure 5. Variation in Gross Cranial Morphology Observed Among Dietary Groupings within the Lake Malawi Haplochromine Radiation

(A–C, left) Arrangements of landmarks used in our analysis illustrated on micro-computed tomographic images of *Astatotilapia calliptera*. Red dots represent landmarks, and yellow dots represent semi-landmarks. Semi-landmarks were

Figure 5. *Continued*

placed at equal distances between landmarks along blue lines. Full explanation of landmark positioning is provided in Figure S2.

(A–C, right) Variation in gross cranial morphology among our 52 study specimens. Variation is shown for each landmark set using canonical variate analysis, displaying canonical variate (CV) scores on the first two axes. Individuals are grouped by diet, and for CV scores, 95% confidence ellipses are shown for all dietary groupings with n > 2. Changes in landmark arrangement associated with each axis are illustrated on wireframe graphs (Klingenberg, 2011). Wireframe graphs along each axis show consensus landmark arrangement for the 52 species (gray dots and lines) and landmark position shifts associated with each CV (black dots and lines). The two wireframe graphs on each axis illustrate changes in landmark positioning associated with the highest and lowest values for each CV on that axis (black dots and lines).

(A) Gross lateral head cranial morphology.

(B) Gross ventral head cranial morphology.

(C) Lower pharyngeal jaw morphology.

ecology, most strikingly by diet (Figures 3A–3C). Collectively these data demonstrate the importance of ecological variables as predictors of both the gross craniofacial morphology and subtle variation in the size and positioning of cranial lateral line canal pores. Our evidence suggests that the cranial lateral line system can adapt readily, like other aspects of trophic morphology, including the lower pharyngeal jaw (Muschick et al., 2012) and oral jaws (Albertson et al., 2003; Albertson and Kocher, 2006; Parsons et al., 2012). We suggest that our findings indicate an important role for the system in facilitating trophic segregation within the wider adaptive radiation context.

Taking an integrated approach will be important for a more robust understanding of the role of the lateral line system in trophic diversification within the radiation. This will include identifying the genetic basis of lateral line system diversity and examining superficial neuromasts alongside canal morphology (Wark and Peichel, 2010; Wark et al., 2012; Becker et al., 2016). To date, research on the genetic basis of lateral line system diversity has focused on superficial neuromasts of the trunk (Becker et al., 2016). Research has identified genes associated with both superficial neuromast morphology and schooling behavior (Wark et al., 2012; Mills et al., 2014; Greenwood et al., 2016). However, identifying the genetic basis for the phenotypic diversity of a system as varied and complex as the cichlid lateral line will be challenging, due to potential epistatic and pleiotropic effects of associated loci (Albertson et al., 2003; Wark et al., 2012; Mills et al., 2014; Greenwood et al., 2016).

In addition, understanding the system's influence on adaptive radiation will require investigating aspects of cichlid behavior and ecology not considered within the scope of this study (Faucher et al., 2010; Stewart et al., 2014; Butler and Maruska, 2015, 2016; York et al., 2018), and evaluating lateral line systems in a multimodal sensory context (Parry et al., 2005; Schwalbe and Webb, 2015). Our findings could extend to other teleost fish radiations, including the cichlid fish radiations of Lake Victoria and Lake Tanganyika. We note that at least one genus in the Lake Tanganyika radiation, *Trematocara*, contains species with enlarged lateral line pores comparable to those of the Lake Malawi *Aulonocara* genus (Takahashi, 2002).

Limitations of the Study

Our study focused on interspecific morphological variability in cranial lateral line morphology, yet ontogenetic variation in cichlid lateral line morphology has been shown in some cichlid species (Bird and Webb, 2014; Webb et al., 2014), and it is possible that sexual dimorphism in morphology may be present if this is associated with ecological factors such as diet. We included one specimen per species in this study, which enabled us to capture broader patterns of interspecific variation. However, a more detailed understanding of intraspecific ontogenetic or sex-associated morphological variation is required.

Our study considered phylogenetic relationships from the perspective of membership of monophyletic clades, as resolved through analyses of whole-genome data (Malinsky et al., 2018). However, whole-genome data are currently not available for all 52 species considered in this study, so we assumed clade membership of some species based on other phylogenetic studies, or knowledge of the phylogenetic placement of congeneric species (Figure S1). In practice, it may not be possible to fully account for phylogenetic history during interspecific analyses across the diversity of cichlids in the Lake Malawi radiation: even with whole-genome data it is not possible to generate a single tree that consistently and adequately resolves all species relationships due to hybridization and incomplete lineage sorting (Malinsky et al., 2018). Finally, the lateral line system is thought to be important for several aspects of species behavior

and ecology we did not consider here, including shoaling behavior (Faucher et al., 2010), aggressive intraspecific interactions (Butler and Maruska, 2015), and habitat light level (Schwalbe et al., 2012). Further comparative work will help to establish whether these factors have additionally contributed to the remarkable diversity we observed.

METHODS

All methods can be found in the accompanying Transparent Methods supplemental file.

SUPPLEMENTAL INFORMATION

Supplemental Information can be found online at https://doi.org/10.1016/j.isci.2019.05.016.

ACKNOWLEDGMENTS

D.E.E. is supported by a NERC GW4+ Doctoral Training Partnership studentship from the Natural Environment Research Council [NE/L002434/1]. We are grateful to Thomas Davies for his assistance with CT scanning and related software.

AUTHOR CONTRIBUTIONS

M.J.G. initially conceived the study and collected the specimens. D.E.E. developed the methods, scanned the specimens, and collected the data. Both authors analyzed the data and wrote the manuscript.

DECLARATION OF INTERESTS

The authors declare no competing interests.

Received: December 13, 2018
Revised: March 6, 2019
Accepted: May 10, 2019
Published: June 28, 2019

REFERENCES

Albertson, R.C., and Kocher, T.D. (2006). Genetic and developmental basis of cichlid trophic diversity. Heredity *97*, 211–221.

Albertson, R.C., Streelman, J.T., and Kocher, T.D. (2003). Genetic basis of adaptive trait differences in the cichlid head. J. Hered. *94*, 291–301.

Becker, E.A., Bird, N.C., and Webb, J.F. (2016). Post–embryonic development of canal and superficial neuromasts and the generation of two cranial lateral line phenotypes. J. Morphol. *277*, 1273–1291.

Bird, N.C., and Webb, J.F. (2014). Heterochrony, modularity and the functional evolution of the mechanosensory lateral line canal system of fishes. EvoDevo *5*, 21.

Bleckmann, H., and Zelick, R. (2009). Lateral line system of fish. Integr. Zool. *4*, 13–25.

Butler, J.M., and Maruska, K.P. (2015). The mechanosensory lateral line is used to assess opponents and mediate aggressive behaviors during territorial interactions in an African cichlid fish. J. Exp. Biol. *218*, 3284–3294.

Butler, J.M., and Maruska, K.P. (2016). Mechanosensory signalling as a potential mode of communication during social interactions in fishes. J. Exp. Biol. *219*, 2781–2789.

Coombs, S., Braun, C.B., and Donovan, B. (2001). The orienting response of Lake Michigan mottled sculpin is mediated by canal neuromasts. J. Exp. Biol. *204*, 337–348.

Cooper, W.J., Parsons, K., McIntyre, A., Kern, B., McGee-Moore, A., and Albertson, C. (2010). Bentho-pelagic divergence of feeding architecture was prodigious and consistent during multiple adaptive radiations within African rift-lakes. PLoS One *3*, e9551.

Eccles, D., and Trewavas, E. (1989). Malawian Cichlid Fishes the Classification of Some Haplochromine Genera (Lake Fish Movies).

Engelmann, J., Hanke, W., Mogdans, J., and Bleckmann, H. (2000). Hydrodynamic stimuli and the fish lateral line. Nature *408*, 51–52.

Faucher, K., Parmentier, E., and Becco, C. (2010). Fish lateral system is required for adequate control of shoaling behaviour. Anim. Behav. *79*, 679–687.

Gelman, S., Avali, A., Tytell, E.D.M., and Cohen, A.H. (2007). Larval lampreys possess a functional lateral line system. J. Comp. Physiol. A Neuroethol. Sens. Neural Behav. Physiol. *193*, 271–277.

Genner, M.J., and Turner, G.F. (2012). Ancient hybridization and phenotypic novelty within Lake Malawi's cichlid fish radiation. Mol. Biol. Evol. *29*, 195–206.

Greenwood, A.K., Mills, M.G., Wark, A.R., Archambeault, S.L., and Peichel, C.L. (2016). Evolution of schooling behaviour in threespine sticklebacks is shaped by the Eda gene. Genetics *2*, 677–681.

Hulsey, C.D., and García de León, F.J. (2005). Cichlid jaw mechanics: linking morphology to feeding specialization. Funct. Ecol. *19*, 487–494.

Janssen, J. (1996). Use of the lateral line and tactile senses in feeding in four Antarctic notothenioid fishes. Env. Biol. Fishes *47*, 51–64.

Klein, A., and Bleckmann, H. (2015). Function of lateral line canal morphology. Integr. Zool. *10*, 111–121.

Klingenberg, C.P. (2011). MorphoJ: an integrated software package for geometric morphometrics. Mol. Ecol. Res. *11*, 353–357.

Klingenberg, C.P. (2013). Visualizations in geometric morphometrics: how to read and how to make graphs showing shape changes. Hystrix It. J. Mamm. *24*, 15–24.

Konings, A. (2016). Malawi Cichlids in Their Natural Habitat, 5th Edition (Cichlid Press).

Kulpa, M., Bak-Coleman, J., and Coombs, S. (2015). The lateral line is necessary for blind cavefish rheotaxis in non-uniform flow. J. Exp. Biol. *218*, 1603–1612.

Legendre, P., and Anderson, M.J. (1999). Distance-based redundancy analysis: testing multispecies responses in multifactorial ecological experiments. Ecol. Monogr. *69*, 1–24.

Malinsky, M., and Salzburger, W. (2016). Environmental context for understanding the iconic adaptive radiation of cichlid fishes in Lake Malawi. Proc. Natl. Acad. Sci. U S A *113*, 11654–11656.

Malinsky, M., Svardal, H., Tyers, A.M., Miska, E.A., Genner, M.J., Turner, G.F., and Durbin, R. (2018). Whole genome sequences of Malawi cichlids reveal multiple radiations interconnected by gene flow. Nat. Ecol. Evol. *2*, 1940–1955.

McKitrick, M.C. (1993). Phylogenetic constraint in evolutionary theory: has it any explanatory power? Annu. Rev. Ecol. Syst. *24*, 307–330.

Mills, M.G., Greenwood, A.K., and Peichel, C.L. (2014). Pleiotropic effects of a single gene on skeletal development and sensory system patterning in sticklebacks. EvoDevo *5*, 5.

Montgomery, J.C., and McDonald, J.A. (1987). Sensory tuning of lateral line receptors in Antarctic fish to the movements of planktonic prey. Science *235*, 195–196.

Montgomery, J.C., Coombs, S., and Janssen, J. (1994). Form and function relationships in lateral line systems: comparative data from six species of Antarctic notothenoid fish. Brain Behav. Evol. *44*, 299–306.

Montgomery, J.C., Baker, C.F., and Carton, A.G. (1997). The lateral line can mediate rheotaxis in fish. Nature *389*, 960–963.

Muschick, M., Barluenga, M., Salzburger, W., and Meyer, A. (2011). Adaptive phenotypic plasticity in the Midas cichlid fish pharyngeal jaw and its relevance to adaptive radiation. BMC Evol. Biol. *11*, 136.

Muschick, M., Indermaur, A., and Salzburger, W. (2012). Convergent evolution within an adaptive radiation of cichlid fishes. Curr. Biol. *22*, 2362–2368.

Parry, J.W., Carleton, K.L., Spady, T., Carboo, A., Hunt, D.M., and Bowmaker, J.K. (2005). Mix and match color vision: tuning spectral sensitivity by differential opsin gene expression in Lake Malawi cichlids. Curr. Biol. *15*, 1734–1739.

Parsons, K.J., Cooper, W.J., and Albertson, R.C. (2011). Modularity of the oral jaws is linked to repeated changes in the craniofacial shape of African cichlids. Int. J. Evol. Biol. *2011*, 641501.

Parsons, K.J., Márquez, E., and Albertson, R.C. (2012). Constraint and opportunity: the genetic basis and evolution of modularity in the cichlid mandible. Am. Nat. *179*, 64–78.

Pohlmann, K., Atema, J., and Breithaupt, T. (2004). The importance of the lateral line in nocturnal predation of piscivorous catfish. J. Exp. Biol. *207*, 2971–2978.

Pugliucci, M. (2008). Is evolvability evolvable? Nat. Rev. Genet. *9*, 75–82.

Salzburger, W. (2018). Understanding explosive diversification through cichlid fish genomics. Nat. Rev. Genet. *19*, 705–717.

Schlosser, G. (2012). Evolution of sensory development – lessons from the lateral line. Brain Behav. Evol. *79*, 73–74.

Schwalbe, M.A.B., and Webb, J.F. (2015). The effect of light intensity on prey detection behaviour in two Lake Malawi cichlids, *Aulonocara stuartgranti* and *Tramatichromis* sp. J. Comp. Physiol. A Neuroethol. Sens. Neural Behav. Physiol. *201*, 341–356.

Schwalbe, M.A.B., Bassett, D.K., and Webb, J.F. (2012). Feeding in the dark: lateral-line-mediated prey detection in the peacock cichlid *Aulonocara stuartgranti*. J. Exp. Biol. *215*, 2060–2071.

Seehausen, O. (2006). African cichlid fish: a model system in adaptive radiation research. Proc. Roy. Soc. Lond. B Biol. Sci. *273*, 1987–1998.

Seehausen, O. (2015). Process and pattern in cichlid radiations–inferences for understanding unusually high rates of evolutionary diversification. New Phytol. *207*, 304–312.

Stewart, W.J., Nair, A., Jiang, H.S., and McHenry, M.J. (2014). Prey fish escape by sensing the bow wave of a predator. J. Exp. Biol. *217*, 4328–4336.

Takahashi, T. (2002). Systematics of the tribe Trematocarini (Perciformes: Cichlidae) from Lake Tanganyika, Africa. Ichthyol. Res. *49*, 253–259.

Turner, G.F. (1996). Offshore Cichlids of Lake Malawi (Cichlid Press).

Wark, A.R., and Peichel, C.L. (2010). Lateral line diversity among ecologically divergent threespine stickleback populations. J. Exp. Biol. *213*, 108–117.

Wark, A.R., Mills, M.G., Dang, L., Chan, Y.H., Jones, F.C., Brady, S.D., Absher, D.M., Grimwood, J., Schmutz, J., Myers, R.M., et al. (2012). Genetic architecture of variation in the lateral line sensory system of threespine sticklebacks. G3 (Bethesda) *2*, 1047–1056.

Webb, J.F. (2014). Morphological diversity, development and evolution of the lateral line system. In The Lateral Line System, S. Coombs, H. Bleckmann, R.R. Fay, and A.N. Popper, eds. (Springer), pp. 17–72.

Webb, J.F., Bird, N.C., Carter, L., and Dickson, J. (2014). Comparative development and evolution of two lateral line phenotypes in lake Malawi cichlids. J. Morphol. *6*, 678–692.

York, R.A., Patil, C., Abdilleh, K., Johnson, Z.V., Conte, M.A., Genner, M.J., McGrath, P.T., Fraser, H.B., Fernald, R.D., and Streelman, J.T. (2018). Behavior-dependent cis regulation reveals genes and pathways associated with bower building in cichlid fishes. Proc. Natl. Acad. Sci. U S A *47*, E11081–E11090.

Young, K.A., Snoeks, J., and Seehausen, O. (2009). Morphological diversity and the roles of contingency, chance and determinism in African cichlid radiations. PLoS One *4*, e4740.

ISCI, Volume *16*

Supplemental Information

Adaptive Diversification of the Lateral Line System during Cichlid Fish Radiation

Duncan E. Edgley and Martin J. Genner

Supplemental Information:

Edgley, D.E. and Genner, M.J. Adaptive diversification of the lateral line system during cichlid fish radiation

Table S1. The specimens used in this study, ordered alphabetically. Related to Figures 2-5.

All specimens collected by M.J. Genner unless otherwise stated. Phylogenetic group derived primarily from Malinsky et al. (2018) (Figure S1). Diet, habitat and depth data primarily from Ribbink *et al*. (1983), Turner (1996), Genner and Turner (2012), Konings (2016), or personal observations. In depth sources of dietary information are listed. Head size is defined as distance from anterior limit of dentary bone to posterior limit of operculum. BI=Benthic Invertebrates; Z=Zooplankton; A=Algae; F=Fish; S=Scales/fins; M=Molluscs. For dietary references: [1] Turner (1996); [2] Konings (2016) [3] Duponchelle *et al*. (2005); [4] Ribbink *et al*. (1983); [5] Hanssens (2004); [6] Genner *et al*., (2007). *Putatively undescribed taxon. **Wild caught by S.M. Grant Ltd, specific location of capture unknown. ***Dietary information derived from personal observations, from examining gut contents or feeding behaviour. †For *Hemitaeniochromis* sp. 'longjaw', diet was assigned based on morphology and the fact that all other *Hemitaeniochromis* species are piscivores/paedophages (From both Turner, 1996 and Konings, 2016).

Species	Collection Date (mm/yy)	Sex	Sampling Location	Diet	Minimum Depth (m)	Maximum Depth (m)	Head Size (mm)	Habitat	Phylogenetic group
Alticorpus peterdaviesi	02/05	M	Monkey Bay, Malawi	BI [1]	50	125	35.78	Soft	Deep Benthic
Astatotilapia calliptera	07/11	M	Lake Itamba, Tanzania	BI***	0	9	25.15	Soft	Mbuna
Aulonocara jacobfreibergi	09/14	M	Cape Maclear, Malawi	BI [1]	2	35	32.20	Hard Cave	Deep Benthic
Aulonocara nyassae	09/14	F	Cape Maclear, Malawi	BI [1]	15	50	27.13	Soft	Deep Benthic
Aulonocara sp. 'copper'	02/05	M	Monkey Bay, Malawi	BI [1]	60	120	34.08	Soft	Deep Benthic
Aulonocara sp. 'yellow collar'	09/14	M	Cape Maclear, Malawi	BI [1]	40	95	25.06	Hard Cave	Deep Benthic
Aulonocara stuartgranti	09/12	M	Unknown**	BI [1]	5	15	33.65	Soft	Deep Benthic
Buccochromis nototaenia	09/14	F	Lake Malombe, Malawi	F [1,2]	18	44	42.63	Soft	Shallow Benthic
Copadichromis chrysonotus	08/14	F	Mangochi, Malawi	Z [1,2]	0	30	29.85	Pelagic	Utaka
Copadichromis cf. *likomae*	09/14	M	Cape Maclear, Malawi	Z [1]	0	30	33.60	Soft	Utaka

Copadichromis virginalis	09/14	M	Cape Maclear, Malawi	Z [1,3]	7	114	29.48	Pelagic	Utaka
Ctenopharynx nitidus	09/14	F	Cape Maclear, Malawi	BI [1,2]	18	65	32.39	Soft	Shallow Benthic
Cynotilapia zebroides	06/97	M	Monkey Bay, Malawi	Z [4]	0	40	20.35	Hard	Mbuna
Dimidiochromis compressiceps	11/11	F	Mangochi, Malawi	F [1,2]	0	10	39.84	Weed	Shallow Benthic
Dimidiochromis dimidiatus	09.14	F	Cape Maclear, Malawi	F [1,2]	0	5	39.71	Soft	Shallow Benthic
Dimidiochromis strigatus	08/14	M	Mangochi, Malawi	F [1,2]	2	10	48.13	Soft	Shallow Benthic
Diplotaxodon greenwoodi	11/04	F	Cape Maclear, Malawi	F [1,2]	50	148	57.53	Pelagic	Diplotaxodon
Diplotaxodon limnothrissa	08/04	M	Cape Maclear, Malawi	Z [1,3]	20	220	40.4	Pelagic	Diplotaxodon
Diplotaxodon sp. 'macrops ngulube'	02/05	M	Nkhata Bay, Malawi	Z [1]	50	100	42.47	Pelagic	Diplotaxodon
Fossarochromis rostratus	06/97	F	Nkhata Bay, Malawi	BI [1,2]	0	10	29.91	Soft	Shallow Benthic
Genyochromis mento	06/97	F	Nkhata Bay, Malawi	S*** [1,2]	0	40	27.07	Hard	Mbuna
Hemitaeniochromis sp. 'longjaw'*	08/14	F	Mangochi, Malawi	F†	35	55	33.35	Soft	Shallow Benthic
Hemitaeniochromis spilopterus	03/05	M	Monkey Bay, Malawi	F [1,2]	28	32	36.45	Soft	Shallow Benthic
Hemitilapia oxyrhynchos	08/14	M	Mangochi, Malawi	A [1,2]	2	20	35.21	Weed	Shallow Benthic
Iodotropheus sprengerae	01/11	F	Chiofu, Malawi	A [2,4]	0	40	18.89	Hard	Mbuna
Labeotropheus trewavasae	09/12	M	Unknown**	A [2,4]	0	34	21.70	Hard	Mbuna
Lethrinops gossei	05/05	M	Tokombo, Malawi	BI [1,3]	46	128	41.97	Soft	Deep Benthic
Lethrinops lethrinus	09/14	M	Lake Malombe, Malawi	BI [1]	0	34	35.72	Soft	Shallow Benthic
Lethrinops sp. 'yellow head'	09/14	M	Cape Maclear, Malawi	BI [1]	40	75	31.47	Soft	Deep Benthic
Lethrinops sp. 'zebra'	05/05	M	Nkhata Bay, Malawi	BI [1]	50	100	34.85	Soft	Deep Benthic
Lichnochromis acuticeps	09/14	F	Cape Maclear, Malawi	F [1,2]	5	15	30.33	Hard	Shallow Benthic
Melanochromis parallelus	06/97	F	Nkhata Bay, Malawi	A [2,4]	0	40	19.70	Hard	Mbuna
Mylochromis anaphyrmus	09/14	F	Cape Maclear, Malawi	M [1,3]	15	72	23.83	Soft	Shallow Benthic
Nimbochromis livingstonii	09/12	M	Unknown**	F [1,2]	2	114	36.42	Hard	Shallow Benthic
Otopharynx tetrastigma	09/14	M	Cape Maclear, Malawi	BI [1,2]	1	7	40.38	Soft	Shallow Benthic
Pallidochromis tokolosh	05/05	M	Kasuza, Malawi	F [1]	50	126	78.42	Pelagic	Diplotaxodon
Placidochromis electra	09/12	F	Unknown**	BI [1,2,5]	0	15	29.44	Soft	Shallow Benthic
Placidochromis milomo	05/05	F	Monkey Bay, Malawi	BI [1,2,5]	4	35	55.92	Hard	Shallow Benthic
Placidochromis platyrhynchos	09/14	M	Cape Maclear, Malawi	BI [1,5]	118	126	30.56	Soft	Deep Benthic
Placidochromis polli	03.05	M	Monkey Bay, Malawi	BI [1,5]	45	128	38.87	Soft	Deep Benthic
Pseudotropheus aurora	09/14	M	Cape Maclear, Malawi	A [4]	3	12	23.77	Hard	Mbuna
Pseudotropheus sp. 'elongatus aggressive'	09/14	M	Cape Maclear, Malawi	A [4]	0	25	20.84	Hard	Mbuna
Rhamphochromis esox	07/04	M	Nkhata Bay, Malawi	F [1,2]	2	65	51.49	Pelagic	Rhamphochromis
Rhamphochromis sp. 'chilingali'	11/04	F	Lake Chilingali, Malawi	F*** [6]	0	100	30.39	Soft	Rhamphochromis
Rhamphochromis sp. 'longiceps grey-back'	02/05	M	Dwangwa, Malawi	F [1]	20	90	51.18	Pelagic	Rhamphochromis

Sciaenochromis psammophilus	10/04	M	Maldeco Fisheries, Malawi	F [1,2]	5	60	46.50	Soft	Shallow Benthic
Stigmatochromis modestus	09/14	F	Cape Maclear, Malawi	F [2]	5	20	34.65	Hard	Shallow Benthic
Stigmatochromis sp. 'guttatus'	06/96	M	Nkhata Bay, Malawi	F [2]	24	100	37.11	Soft	Shallow Benthic
Taeniochromis holotaenia	09/14	F	Cape Maclear, Malawi	F [1,2]	15	64	31.70	Soft	Shallow Benthic
Taeniolethrinops praeorbitalis	08/14	F	Mangochi, Malawi	BI [1,3]	2	55	54.82	Soft	Shallow Benthic
Trematocranus placodon	04/05	M	Monkey Bay, Malawi	M [1,2]	2	20	41.89	Soft	Shallow Benthic
Tyrannochromis macrostoma	06/97	M	Nkhata Bay, Malawi	F [1,2]	0	40	37.52	Hard	Shallow Benthic

Table S2. Scanning information for all 52 species, and all 14 scans. Related to Figures 1-5.

Scans were carried out in two sessions, on the 23rd January 2017 and 6th February 2017. The scanner used was a Nikon XTH225ST system in the Life Sciences Building at the University of Bristol. Each scan lasted 45-60 minutes.

Scan	Species	Analysis order	Species ID	Scan Voxel Size (mm)	X-ray kV	X-ray µA	X-ray mW	No. projections	Date of scan
DELL16-01_LOWER	*Dimidiochromis compressiceps*	13	213	0.067	130	230	29900	3141	06/02/2017
	Aulonocara jacobfreibergi	2	123						
	Lethrinops lethrinus	27	185						
	Melanochromis parallelus	32	MP						
DELL16-01_UPPER	*Aulonocara nyassae*	3	134	0.064	130	230	29900	3141	06/02/2017
	Copadichromis virginalis	10	152						
	Stigmatochromis sp. 'guttatus'	45	SG						
	Nimbochromis livingstonii	33	NL						
DELL16-02_LOWER	*Taeniochromis holotaenia*	48	111	0.066	130	205	26650	3141	06/02/2017
	Lichnochromis acuticeps	25	130						
	Placidochromis platyrhynchos	39	160						
	Stigmatochromis modestus	46	118						
DELL16-02_UPPER	*Buccochromis nototaenia*	7	175	0.068	130	205	26650	3141	06/02/2017
	Ctenopharynx nitidus	9	135						
	Lethrinops sp. 'yellow head'	29	164						
	Labeotropheus trewavasae	28	LT						
DELL16-03_LOWER	*Genyochromis mento*	20	200	0.068	130	235	30500	3141	23/01/2017
	Tyrannochromis macrostoma	49	201						
	Fossorochromis rostratus	19	202						
	Rhamphochromis sp. 'chilingali'	42	203						
DELL16-03_UPPER	*Cynotilapia zebroides*	11	204	0.081	130	225	29250	3141	23/01/2017
	Diplotaxodon sp. 'macrops ngulube'	17	205						
	Placidochromis milomo	38	206						
DELL16-04_LOWER	*Diplotaxodon limnothrissa*	16	207	0.074	130	225	29250	3141	23/01/2017

	Lethrinops sp. ‘zebra’	30	209						
	Mylochromis anaphyrmus	31	132						
	Pseudotropheus sp. 'elongatus aggressive'	37	129						
DELL16-04_UPPER	*Placidochromis polli*	40	210	0.074	130	225	29250	3141	23/01/2017
	Hemitaeniochromis sp. 'longjaw'	21	33						
	Copadichromis chrysonotus	12	32						
	Hemitaeniochromis spilopterus	23	211						
DELL16-05_LOWER	*Diplotaxodon greenwoodi*	15	215	0.073	130	205	26650	3141	06/02/2017
	Otopharynx tetrastigma	34	217						
	Trematocranus placodon	50	220						
	Copadichromis cf. *likomae*	8	167						
DELL16-05_UPPER	*Iodotropheus sprengerae*	24	214	0.064	130	205	26650	3141	06/02/2017
	Astatotilapia calliptera	0	218						
	Aulonocara stuartgranti	5	219						
	Dimidiochromis dimidiatus	14	162						
DELL16-06_LOWER	*Pseudotropheus aurora*	35	159	0.068	130	205	26650	3141	06/02/2017
	Aulonocara sp. ‘yellow collar’	6	144						
	Hemitilapia oxyrhynchos	22	40						
	Placidochromis electra	36	221						
DELL16-06_UPPER	*Sciaenochromis psammophilus*	47	222	0.068	130	205	26650	3141	06/02/2017
	Alticorpus peterdaviesi	4	223						
	Aulonocara sp. ‘copper’	1	224						
	Lethrinops gossei	26	225						
DELL16-09	*Dimidiochromis strigatus*	18	39	0.085	130	220	28600	3141	06/02/2017
	Taeniolethrinops praeorbitalis	51	31						
	Rhamphochromis sp. 'longiceps grey-back’	44	212						
	Rhamphochromis esox	43	208						
DELL16-10	*Pallidochromis tokolosh*	41	216	0.076	130	205	26650	3141	06/02/2017

Figure S1. A cladogram for the 52 species included in our study, based primarily on Malinsky *et al*. (2018), coloured by diet. Related to Figures 2-5.

*Grouping assigned based on systematic evidence from congenerics (19/52 cases). *Aulonocara* species and the deep water *Lethrinops* were assigned to the deep benthic group based on both morphology and evidence from mtDNA (Genner and Turner 2012; Konings, 2016; Malinsky *et al*., 2018). *Labeotropeus trewavasae* and *Lichnochromis acuticeps* were assigned to the mbuna and shallow benthic groups respectively based on Genner and Turner (2012). *Melanochromis parallelus* was assigned as mbuna based on congeneric *Melanochromis elastodema* (Genner and Turner, 2012).

Pseudotropheus aurora and *Pseudotropheus* sp. ‘elongatus aggressive’ were assigned to mbuna based on the congeneric *Pseudotropheus acei* (Joyce *et al*. 2011; Malinsky *et al*. 2018). *Hemitaeniochromis* sp. ‘longjaw’ was assigned to shallow benthic based on congeneric *Hemitaeniochromis spilopterus* (Malinsky *et al*. 2018). *Sciaenochromis psammophilus* was assigned as shallow benthic based on congeneric *Sciaenochromis benthicola* (Genner and Turner, 2012). *Tyrannochromis macrostoma* was assigned as shallow benthic based on congeneric *Tyrannochromis nigriventer* (Malinsky *et al*. 2018).

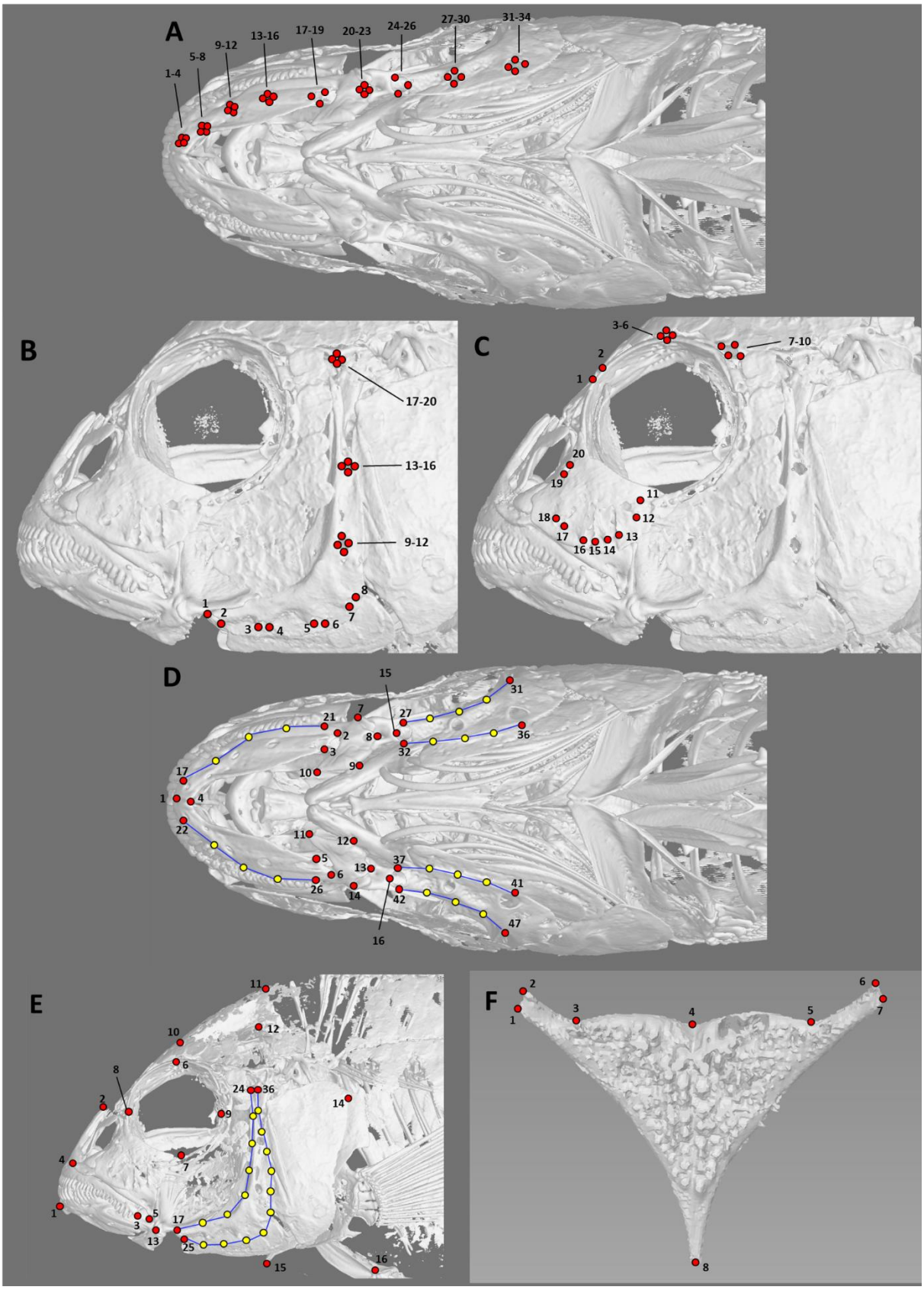

Figure S2. Landmark configurations used in this study, illustrated on 2D images from microCT reconstructions of *Astatotilapia calliptera*. Related to Figures 3-5.

Red dots are landmarks and yellow dots are sliding semi-landmarks. Semi-landmarks are placed at equal distance between landmarks along blue lines. Semi-landmarks were digitised at equal distance between the two landmarks, and were converted to landmarks for analysis. (A) Ventral head lateral line pore landmarks. Groups of 4 landmarks were digitised in the following order: left pore limit; right pore limit; anterior pore limit; posterior pore limit. 17-19 were digitised: left pore limit; anterior pore limit; right pore limit. 24-26 were digitised: left pore limit; posterior pore limit; right pore limit. (B) Preopercular lateral line pore landmarks. Groups of 4 landmarks were digitised as follows: dorsal pore limit, ventral pore limit, anterior pore limit, posterior pore limit. (C) Orbital lateral line pore landmarks. Groups of 4 landmarks were digitised as follows: anterior pore limit, posterior pore limit, dorsal pore limit, ventral pore limit. (D) Gross ventral head landmarks. Structures referred to as being 'left' are on the upper half, and those referred to as 'right' are on the lower half. 1: anterior limit of meeting point of left and right dentary bones; 2: posterior outer limit of right dentary bone; 3: Posterior inner limit of right dentary bone; 4: posterior limit of meeting point of left and right dentary bones; 5: posterior inner limit of left dentary bone; 6: posterior outer limit of left dentary bone; 7: right-most limit of right angulo-articular bone; 8: posterior limit of right angulo-articular bone; 9: posterior limit of inner edge of right angulo-articular bone; 10: anterior limit of right angulo-articular bone; 11: anterior limit of left angulo-articular bone; 12: posterior limit of inner edge of left angulo-articular bone; 13: posterior limit of left angulo-articular bone; 14: left-most limit of left angulo-articular bone; 17-21: Sliding landmarks along outer edge of right dentary bone, from in line with midpoint of anterior-most right dentary pore (17) to in line with midpoint of posterior-most right dentary pore (21); 22-26: Sliding landmarks along outer edge of left dentary bone, from in line with midpoint of anterior-most left dentary pore (22) to in line with midpoint of posterior-most left dentary pore (26); 27-31: Sliding landmarks along outer edge of right preoperculum, from in line with midpoint of anterior-most right preopercular pore (27) to in line with midpoint of 3rd anterior-most right preopercular pore (31); 32-36: Sliding landmarks along inner edge of right preoperculum from in line with midpoint of anterior-most right preopercular pore (32) to in line with midpoint of 3rd anterior-most right preopercular pore (36); 37-41: Sliding landmarks along inner edge of left preoperculum from in line with midpoint of anterior-most left preopercular pore (37) to in line with

midpoint of 3rd anterior-most left preopercular pore (41); 42-47: Sliding landmarks along outer edge of left preoperculum from in line with midpoint of anterior-most left preopercular pore (42) to in line with midpoint of 3rd anterior-most left preopercular pore (47). (E) Gross lateral head landmarks. 1: anterior limit of dentary bone; 2: dorsal limit of premaxilla; 3: posterior limit of oral cavity; 4: ventral limit of premaxilla; 5: Joint of angulo-articular and quadrate; 6: dorsal limit of bony orbit; 7: ventral limit of bony orbit; 8: anterior limit of bony orbit; 9: posterior limit of bony orbit; 10: anterior limit of supraoccipital crest; 11: dorsal limit of supraoccipital crest; 12: posterior ventral point of supraoccipital crest; 13: anterior limit of quadrate; 14: posterior limit of operculum; 15: anterior limit of cleithrum; 16: posterior limit of pelvic girdle; 17-24: sliding landmarks along dorsal/anterior edge of preoperculum; 25-36: sliding landmarks along ventral/posterior edge of preoperculum. (F) Lower pharyngeal jaw landmarks followed Muschick *et al.* 2011.

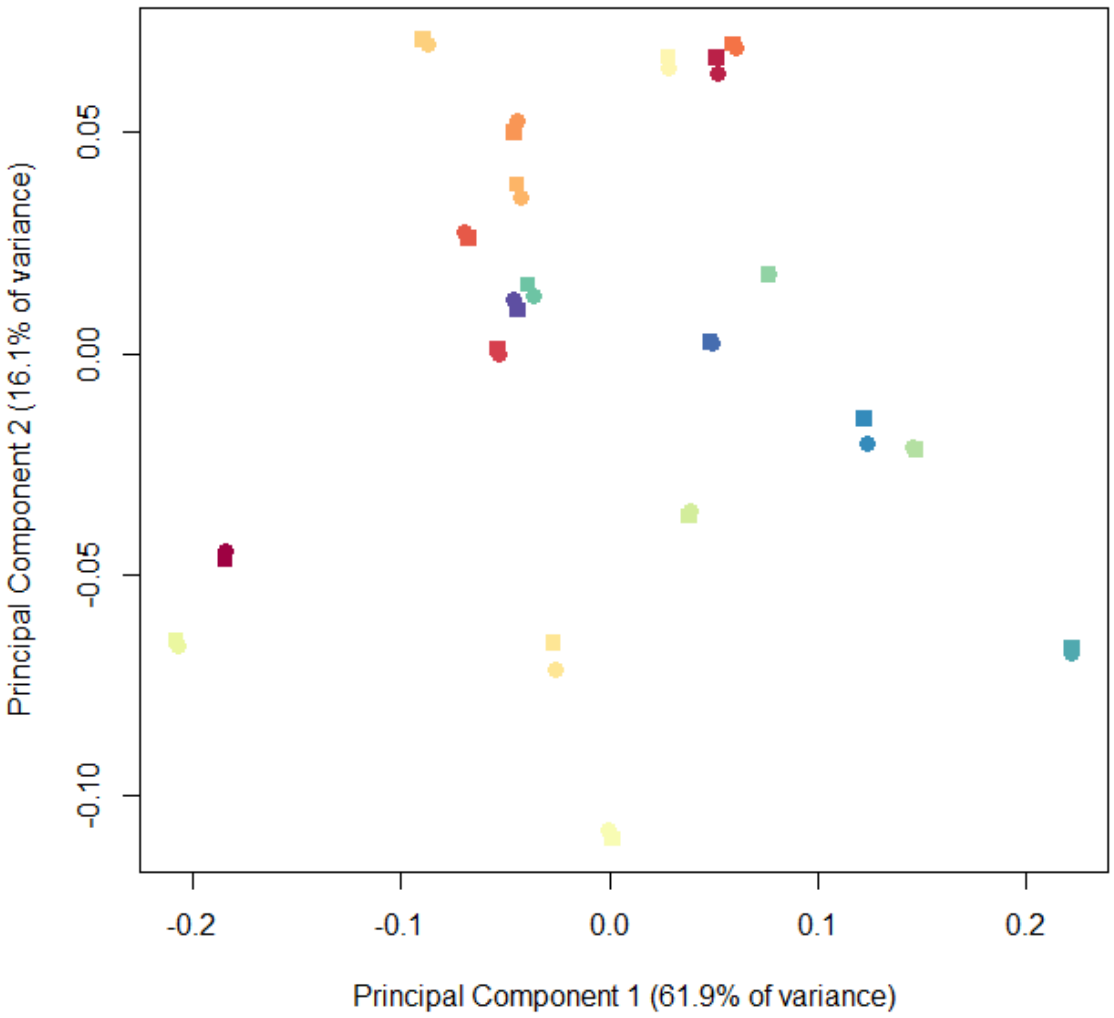

Figure S3. Principal Component Analysis of gross lateral head landmarks of individuals subjected to repeated landmarking. Related to Figures 3-5.

Landmarks used are shown in Figure S1E. Landmark data was aligned using Procrustes analysis. Shapes indicate landmarking event (square = original, repeat = circle), while each colour represents a separate individual (=species).

Transparent Methods

Contact for reagent and resource sharing

Further information and requests for resources and files should be directed to and will be fulfilled by Duncan Edgley (duncan.edgley@bristol.ac.uk).

Experimental model and subject details

Our study included one specimen from each of 52 cichlid species from the Lake Malawi catchment (Lake Malawi, Lake Malombe, Lake Itamba and Lake Chilingali), collected between 1997 and 2014 (Table S1). Specimens were chosen to represent the phylogenetic, morphological and ecological diversity within the flock (Genner and Turner, 2012; Konings, 2016; Malinsky *et al*., 2018). Species from all major trophic groups, habitats and depths were included in the sample set (Turner, 1996; Konings, 2016) (Table S1). Specimens had been fixed in either formalin or ethanol in the field, and later transferred to 70% ethanol.

This study focusses on larger patterns of interspecific variation across the Lake Malawi species flock, and like equivalent studies of other aspects of morphological variation in adaptive radiations we use one representative individual of each species (Young *et al*., 2009; Cooney *et al.*, 2018). We note that by including one only specimen of each species, we do not capture intraspecific variation, and that use of more specimens would have increased the precision of our estimates.

MicroCT Scans and 3D Reconstructions

A Nikon XTH225ST microCT scanning system was used to generate the images. In total fourteen scans were conducted, each lasting approximately 45 minutes. Each scan used 3141 projections and included between three and six individuals (Table S2). Scan resolution was determined by the size of the region of interest for each scan, which in term was determined by specimen size. There was a trade-off between

scan resolution and the size and number of specimens in each scan. To optimise resolution, we conducted preliminary scans and carefully observed that the smallest structures of interest (lateral line canal pores, and orbital bones) were visible in each slice. We concluded that a voxel size of 60-80µm was adequate for the desired analysis. Image stacks from the scans were exported into VG Studio 3.0 (Volume Graphics GmbH, 2016) and reconstructed into a 3D model of each specimen. From these 3D reconstructions, we captured 2D images from the ventral head perspective (Figures S2A and D) and lateral head perspective (Figure S2B and E). We used Avizo 8.0 (Hillsboro, OR) to isolate the lower pharyngeal jaw (LPJ) from the rest of the skeleton, and images of the resulting isolated LPJs were captured from the dorsal perspective (Figure S2F). The LPJ was included in our analysis to: i) test the expected relationship between diet and LPJ morphology previously shown in Tanganyika cichlids (Muschick *et al*., 2011), and ii) provide a method of evaluating the ability our analytical approach to resolve associations between morphology and ecological variables.

Landmark Digitisation

Lateral line canal landmarks were chosen to capture information on the size and distribution of pores in the cranial lateral line canal system (Figure S2A-C). Some cranial canal pores could not be seen clearly enough to be consistently and accurately landmarked in all 52 scans (such as pores of the post-otic and supratemporal canals) and were therefore omitted. To ensure the number of landmarks did not exceed the sample size (Webster and Sheets, 2010), we only digitised the pores on one side of the fishes' heads when quantifying ventral head lateral line pore morphology, as illustrated in Figure S2A. Gross skeletal morphology landmarks (Figure S2E) were chosen to reflect elements with relevance to the lateral line system, for example the shape of the dentary bones and the preoperculum. Skeletal elements were chosen which were clearly visible on all species and all qualities of scan. To capture the shape of curved elements such as the preoperculum and the dentary bones, we appended equidistant sliding semi-landmarks to curves between two landmarks. For analysis purposes these were converted to landmarks in tpsUtil64 1.74 (SUNY Stony Brook, NY). Landmarks used for comparing LPJ morphology followed Muschick *et al.*, 2011 (Figure S2F).

Landmarks and semi-landmarks were digitised using tpsDig2 2.30 for Windows (SUNY Stony Brook, NY), using the images exported from VG Studio 3.0. Image files were constructed using tpsUtil64 1.74, as was conversion of semi-landmarks to landmarks, and construction of slider files (to specify the identity of semi-landmarks). Semi-landmarks were converted to landmarks in tpsUtil64 1.74 for analysis in MorphoJ 2.0 (Klingenberg, 2011). Through Procrustes analysis, we accounted for the effect of rotation, translation and scaling. In instances where pores appeared closed, yet the location was still typically discernible, and four landmarks were placed on top of each other. In total we had six sets of landmarks to digitise, with each set comprising 52 images. Each landmark set was digitised in one session, and by the same person (D. Edgley).

Ecological data collection

Ecological variables with potential associations with craniofacial morphology were chosen, including diet, substrate type and depth (Turner, 1996; Konings 2016). Species were assigned to one of six primary dietary classes: benthic algivore, benthic arthropod feeder, zooplanktivore, molluscivore, piscivore and scale eater/fin biter (Ribbink *et al*., 1983; Turner, 1996; Hassens, 2004; Duponchelle *et al*., 2005; Hanssens, 2004; Genner *et al*., 2007; Konings 2016). They were also assigned one of five primary habitats: soft substrate, hard substrate, weed, cave and pelagic (Turner, 1996; Konings 2016). Minimum and maximum depth was derived from the literature (Ribbink *et al*., 1983; Turner, 1996; Genner and Turner, 2012; Konings, 2016) or given as best estimate from personal observations (M. Genner) where literature was unavailable. We also assigned species to one of six major phylogenetic groupings: *Diplotaxodon-Pallidochromis*; mbuna (including *Astatotilapia calliptera*); *Rhamphochromis*; utaka; deep-benthic; and shallow-benthic (Genner and Turner, 2012; Malinsky *et al*., 2018) (Figure S1). Ecological variables are summarized in Table S1.

Quantification and statistical analysis

We carried out a Procrustes fit on each set of landmarks, aligned by principal axes in MorphoJ 2.0 (Klingenberg, 2011). Raw Procrustes coordinates were then standardised (mean = 0, SD = 1). Distance-based redundancy analyses (dbRDA) were used to investigate relative strengths of association between predictor variables (diet, habitat, minimum depth, maximum depth, phylogenetic grouping, and the relevant morphological variables) and cranial lateral line canal pore morphology (Legendre and Anderson, 1999) (Figure 3). Data (categorical ecology variables, phylogenetic grouping and standardised Procrustes coordinates) were converted to dissimilarity matrices in PAST 3.15 (Oslo). The package "vegan 2.4-3" was used to carry out the analysis in R 2.15.1 for Windows (R Core team, 2012) (Oksanen *et al*., 2017): Head size, minimum depth and maximum depth were imputed as continuous variables. We used the ordistep procedure to identify the optimal model, using default settings. Significance tests were carried out with 10,000 permutations. To ordinate morphological variables in relation to ecological grouping, we used Canonical Variate Analysis (CVA), in MorphoJ (Figure 4; Figure 5) (Klingenberg, 2011). To visualise changes in landmark placement associated with each canonical variate in relation to consensus landmark arrangement, we constructed wireframe graphs in MorphoJ (Figure 4; Figure 5) (Klingenberg, 2011; Klingenberg, 2013). To test for landmark digitization error, we re-digitised 20 individuals using gross lateral head landmarks (Figure S2E). We then performed a Procrustes alignment using the R package "geomorph" (Adams *et al*., 2018), followed by a Principal Component Analysis on the Procrustes coordinates. We quantified differences among species and landmarking events (original vs. repeat) using Analysis of Variance using R on each of the two main Principal Component axes, that collectively captured 78.1% of the variance. We found highly significant differences between species (PC1, $F_{(19, 19)} = 20391.93$, $P < 0.001$; PC2, $F_{(19,19)} = 1824.47$, $P < 0.001$), but not between landmarking events (PC1, $F_{(1, 19)} = 1.017$, $P = 0.326$; PC2, $F_{(1,19)} = 1.931$, $P = 0.181$) (Figure S4).

Supplementary Material References:

Adams, D.C., Collyer, M.L., and Kaliontzopoulou, A. (2018). Geomorph: Software for geometric morphometric analyses. R package version 3.0.6. https://cran.r-project.org/package=geomorph.

Cooney, C.R., Bright, J.A., Capp, E.J., Chira, A.M., Hughes, E.C., Moody, C.J., Nouri, L.O., Varley, Z.K. and Thomas, G.H. (2017). Mega-evolutionary dynamics of the adaptive radiation of birds. Nature 542, 344-347.

Duponchelle, F., Ribbink, A.J., Msukwa, A., Mafuka, J., Mandere, D., and Bootsma, H. (2005) Food partitioning within the species-rich benthic fish community of Lake Malawi, East Africa. Can. J. Fish. Sci. Aquat. 62, 1651-1664.

Genner, M.J., and Turner, G.F. (2012) Ancient hybridization and phenotypic novelty within Lake Malawi's cichlid fish radiation. Mol. Biol. Evol. 26, 195-206.

Genner, M.J., Nichols, P., Carvalho, G.R., Robinson, R.L., Shaw, P.W., Smith, A., and Turner, G.F. (2007) Evolution of a cichlid fish in a Lake Malawi satellite lake, Proc. Roy. Soc. Lond. B - Biol. Sci. 1623, 2249-2257.

Hanssens, M. (2004) Chapter 7: The deep-water Placidochromis species. In The cichlid diversity of Lake Malawi/Nyassa/Niassa: identification, distribution and taxonomy, ed. Snoeks, J (Cichlid Press), 104-197.

Joyce, D.A., Lunt, D.H., Genner, M.J., Turner, G.F., Bills, R. and Seehausen, O. (2011). Repeated colonization and hybridization in Lake Malawi cichlids. Curr. Biol. 21, R108-R109.

Klingenberg, C.P. (2011). MorphoJ: an integrated software package for geometric morphometrics. Mol. Ecol. Res. 11, 353-357.

Klingenberg, C.P. (2013) Visualizations in geometric morphometrics: how to read and how to make graphs showing shape changes. Hystrix It. J. Mamm. 24, 15-24.

Konings, A. (2016). Malawi cichlids in their natural habitat, 5th Edition (Cichlid Press)

Legendre, P., and Anderson, M.J. (1999). Distance-based redundancy analysis: testing multispecies responses in multifactorial ecological experiments. Ecol. Mono. 69, 1-24.

Malinsky, M., Svardal, H., Tyers, A.M., Miska, E.A., Genner, M.J., Turner, G.F., and Durbin, R. (2018). Whole genome sequences of Malawi cichlids reveal multiple radiations interconnected by gene flow. Nat. Ecol. Evol. 2, 1940–1955.

Muschick, M., Barluenga, M., Salzburger, W., and Meyer, A. (2011). Adaptive phenotypic plasticity in the Midas cichlid fish pharyngeal jaw and its relevance to adaptive radiation. BMC Evol. Biol. 11, 136.

Oksanen, J., Blanchet, F., Friendly, M., Kindt, R., Legendre, P., McGlinn, D., Minchin, P.R., O'Hara, R.B., Simpson, G.L., Solymos, P. et al. (2017). vegan: community ecology package, R package version 2.4-2.

Rambaut, A. (2018) Figtree v1.4.4. http://tree.bio.ed.ac.uk/software/*figtree*/

Ribbink, A.J., Marsh, B.A., Marsh, A.C., Ribbink, A.C., and Sharp, B.J. (1983) A preliminary survey of the cichlid fishes of rocky habitats in Lake Malawi, S. Afr. J. Zool. 18, 149-310.

Turner, G.F. (1996). Offshore cichlids of Lake Malawi, First Edition (Cichlid Press)

Webster, M., and Sheets, D.H. (2010). A practical introduction to landmark-based geometric morphometrics. Quantitative methods in Palaeobiology. The Palaeontological Society Papers 16, 163-188.

Young, K.A., Snoeks, J. and Seehausen, O. (2009) Morphological diversity and the roles of contingency, chance and determinism in African cichlid radiations. PLoS ONE 4, e4740.